# Appendix V

Korhonen, S. T., Airaksinen, S. M. K., Bañares, M. A., Krause, A. O. I., Isobutane dehydrogenation on zirconia-, alumina-, and zirconia/alumina-supported chromia catalysts, *Appl. Catal. A* **333** (2007) 30–41. DOI: 10.1016/j.apcata.2007.08.040.

Available online at www.sciencedirect.com
ScienceDirect
Applied Catalysis A: General 333 (2007) 30–41
APPLIED CATALYSIS A: GENERAL
www.elsevier.com/locate/apcata

# Isobutane dehydrogenation on zirconia-, alumina-, and zirconia/alumina-supported chromia catalysts

Satu T. Korhonen [a,*], Sanna M.K. Airaksinen [a], Miguel A. Bañares [b], A. Outi I. Krause [a]

[a] *Helsinki University of Technology, Department of Chemical Technology, Laboratory of Industrial Chemistry, Kemistintie 1, P.O. Box 6100, FI-02015 TKK, Finland*
[b] *Instituto de Catalisis y Petroleoquimica, CSIC, Campus Cantoblanco, E-28049 Madrid, Spain*

Received 3 August 2007; received in revised form 31 August 2007; accepted 31 August 2007
Available online 6 September 2007

**Abstract**

The performances of zirconia-, alumina-, and zirconia/alumina-supported chromia catalysts were investigated in the dehydrogenation of isobutane in order to elucidate the role of the support material in the dehydrogenation reaction. The dehydrogenation reaction was studied by activity measurements and by experiments using in situ diffuse reflectance infrared Fourier transform spectroscopy (DRIFTS) and in situ Raman spectroscopy. Zirconia was deposited on alumina to clarify if it is possible to combine the beneficial properties of the industrially used chromia/alumina catalysts with those of the more active chromia/zirconia. Zirconia deposition on alumina decreased the Lewis acidity of the support and the coke formation rate during the dehydrogenation. The dehydrogenation activities of the supports were low. Deposition of chromium (1–2 $at_{Cr}/nm^2$) increased the activity for all catalysts. The chromia/zirconia catalyst had the highest activity, whereas the use of zirconia/alumina support decreased the activity. The coke deposition rate increased with increasing dehydrogenation activity. The results suggested that the Lewis acidity alone is not important for the activity of the chromia-containing catalysts, but the phase of zirconia might have an influence.


*Keywords:* Dehydrogenation; Infrared; Raman; Chromia; Zirconia; Alumina

## 1. Introduction

Catalytic dehydrogenation with chromia/alumina is an industrially important route for producing light alkenes [1]. This system has been extensively studied during the past decades [2–7]. The activity of the chromia dehydrogenation catalysts can be enhanced, e.g. by adding alkali dopants [8], or by the use of zirconia as the support material [9]. Zirconia, however, despite its beneficial influence on the dehydrogenation activity, suffers from a low surface area. Therefore, zirconia has been deposited on high surface area oxides such as alumina to prepare zirconia supports with high surface area [10–15].

The surface composition and characteristics of zirconia/alumina have been studied to some extent. Zirconia has been deposited on alumina by impregnation from solution [10–12,14], and by atomic layer deposition (ALD) [13], which was previously known as atomic layer epitaxy (ALE). Pure, bulk zirconia exhibits three well-defined crystal phases of which the monoclinic phase (stable below ~1100 °C [16]) is commonly used for, e.g. catalytic applications. The monoclinic phase transforms into the tetragonal (stable below ~2400 °C) and the cubic (stable below the melting point of ~2670 °C) phases with increasing temperature [16].

The monolayer capacity of zirconia on alumina (calculated based on the surface area of the support) has been estimated to be 4–5 $at_{Zr}/nm^2$ [13] or even 7.4 $at_{Zr}/nm^2$ [12]. Below the monolayer coverage zirconia is amorphous, whereas at higher loadings nano-sized tetragonal zirconia crystallites or islands of these crystallites are formed [10,13,14]. Especially at low loadings, zirconia has also been suspected to migrate into the alumina matrix forming a mixed oxide [10–12]. Earlier, we

* Corresponding author. Tel.: +358 9 451 2618; fax: +358 9 451 2622.
*E-mail addresses:* satu.korhonen@tkk.fi (S.T. Korhonen), sanna.airaksinen@tkk.fi (S.M.K. Airaksinen), banares@icp.csic.es (M.A. Bañares), outi.krause@tkk.fi (A.O.I. Krause).

0926-860X/$ – see front matter © 2007 Elsevier B.V. All rights reserved.
doi:10.1016/j.apcata.2007.08.040

have investigated by methanol adsorption–desorption experiments [17] the Lewis acidic, redox, and basic characteristics of zirconia/alumina-supported chromia catalysts in comparison with the zirconia- and alumina-supported catalysts. The results suggested a strong interaction between the deposited zirconia and the support alumina, although the formation of a mixed oxide was not observed. Furthermore, zirconia/alumina behaved more like alumina than zirconia.

The possible oxidation states of chromium on inorganic oxides are +2, +3, +5, and +6, but their occurrence depends on the catalyst preparation and pretreatment conditions, and the chromium content [3]. The monolayer coverage of chromium on alumina is approximately 4–5 $at_{Cr}/nm^2$ [1,4,5]. On zirconia the monolayer coverage has been estimated to be 5 $at_{Cr}/nm^2$ [9] or even 9 $at_{Cr}/nm^2$ [4]. $Cr^{6+}$ species dominate on alumina under oxidizing conditions at low surface densities of chromium (up to ~0.5 $at_{Cr}/nm^2$), and traces of $Cr^{5+}$ (1–2% of total chromium [9]) can also be detected. On zirconia comparable amounts of $Cr^{5+}$ (50% of total chromium) and $Cr^{6+}$ are present at low surface densities [9]. At low surface densities the chromium species are mainly monochromates [1]. At an intermediate coverage $Cr^{3+}$ species are also present and the fraction of polychromates increases with increasing coverage [1,9]. Above the monolayer coverage on both oxides crystalline $\alpha$-$Cr_2O_3$ is formed and the main oxidation state is +3, but $Cr^{6+}$ species are also present [1,9].

On alumina the high oxidation state species reduce in the presence of alkanes, hydrogen, and carbon monoxide to produce $Cr^{3+}$ and possibly some $Cr^{2+}$ [1,6,7]. According to De Rossi et al. [9] on zirconia the $Cr^{6+}$ and $Cr^{5+}$ species reduce under carbon monoxide to $Cr^{2+}$ and $Cr^{3+}$ species, respectively. The catalytically active species in the dehydrogenation reaction on chromia/alumina and chromia/zirconia are the $Cr^{3+}$ species available to the alkane molecules [1,3,6,7,9]. De Rossi et al. [9] assigned the higher dehydrogenation activity of chromia/zirconia compared with chromia/alumina to the high concentration of mononuclear $Cr^{5+}$ species that reduce under reaction conditions to form mononuclear $Cr^{3+}$ species. However, for chromia/alumina the dehydrogenation activity is insensitive to the size of the $Cr^{3+}$ species and their redox history [7].

The catalytic performance of zirconia/alumina-supported catalysts has been investigated in the reforming reaction of methane with carbon dioxide [14], in the dehydrogenation of isobutane [15], and in the combustion of methane and in the reduction of nitrogen oxide [18]. Souza et al. [14] observed an increase in the reforming activity of zirconia/alumina-supported platinum catalysts in comparison to zirconia- and, especially, alumina-supported ones. The zirconia/alumina catalysts showed a high activity in a wide temperature range, whereas the alumina- and zirconia-supported catalysts were only active either at low or at high temperature, respectively. In addition, the zirconia/alumina catalysts had a similar, high resistance to coke formation as the zirconia-supported catalyst had. Gaspar and Dieguez [15] observed a slight increase in the activity of a chromia catalyst in the dehydrogenation of isobutane when using zirconia/alumina as the support material instead of alumina. However, Burch and Loader [18] observed a lower activity for the zirconia/alumina-supported rhodium catalysts in the combustion of methane and in the reduction of nitrogen oxide compared with zirconia- or alumina-supported ones, respectively. According to them this was due to the incomplete monolayer of zirconia on alumina that interfered but not fully prevented the interaction of rhodium with alumina on these catalysts modifying the active surface species.

In the present study the activity and behavior of chromia/zirconia/alumina catalysts is compared with that of both chromia/alumina and chromia/zirconia. The aim of this study was to elucidate the role of the support material in the dehydrogenation reaction. The catalysts were studied by in situ DRIFTS and in situ Raman spectroscopy which give information on the surface species formed under reaction conditions. Earlier obtained acid–base properties [17] and the surface species formed under isobutane were correlated with activity results. The chromia catalysts and the zirconia/alumina supports were prepared by ALD, where the deposition occurs through self-terminating and saturating gas–solid reactions ensuring a high dispersion and homogeneity of the material [13,19]. Thereby, the samples were more homogenous and similar surface chromium densities were present independent of the support material enabling the conclusions on the role of the support material on the dehydrogenation performance.

## 2. Experimental

### 2.1. Sample preparation and characterization

The supports and the chromia catalysts used in the study are summarized in Table 1. The samples are referred to as *x*(*y*)*CrZ*,

Table 1
The catalyst characteristics determined by BET, XRF, and UV–vis techniques

| Sample | Description | SA ($m^2/g$) | wt.% Cr | $at_{Cr}/nm^2$ | $at_{Cr}^{6+}/nm^2$ | wt.% Zr | $at_{Zr}/nm^2$ |
|---|---|---|---|---|---|---|---|
| $Al_2O_3$ | Alumina | 185 | – | – | – | – | – |
| $ZrO_2$ | Zirconia | 47 | – | – | – | n.a.[a] | n.a.[a] |
| 4.4ZrAl | Zirconia/alumina | 165 | – | – | – | 4.4 | 1.7 |
| 15ZrAl [13] | Zirconia/alumina | 150 | – | – | – | 15 | 5.2 |
| 0.8CrZr | Chromia/zirconia | 48 | 0.8 | 1.9 | 1.1 | n.a.[a] | n.a.[a] |
| 2.2CrAl | Chromia/alumina | 181 | 2.2 | 1.4 | 1.1 | – | – |
| 2.0(4.4)CrZrAl | Chromia/zirconia/alumina | 169 | 2.0 | 1.4 | 0.8 | 4.4 | 1.7 |
| 2.1(15)CrZrAl | Chromia/zirconia/alumina | 148 | 2.1 | 1.6 | 1.2 | 15 | 5.2 |

[a] n.a.: not analyzed.

where $x$ is the amount of chromium in wt.%, $y$ is the amount of zirconium in wt.%, and $Z$ is the support (Zr for zirconia, Al for alumina, or ZrAl for zirconia/alumina). The preparation and some of the characterizations of the catalysts are described in detail in our earlier publication [17].

Commercial zirconia (Mel Chemicals EC 0100 1/8 in) and alumina (Akzo 000-1.5 E, γ-alumina) supports were used in the study. The supports were calcined in air before use at 600 °C for 16 h. The zirconia/alumina supports were prepared by ALD using $ZrCl_4$ (Fluka 98%) as the zirconium precursor. During the preparation the precursor reacts with the surface species of the support forming a complex that still contains some of the chlorine ligands [13,19]. The surface complexes were decomposed to form zirconia by using water vapour at elevated temperature. Two zirconia/alumina supports were prepared using one or five sequences of complex formation and water vapour treatment. The supports contained zirconium either below, or approximately equal to the monolayer coverage of ~4 $at_{Zr}/nm^2$ [13]. The zirconia/alumina supports were calcined in air at 600 °C for 16 h. The ALD preparation of zirconia/alumina is described in more detail by Kytökivi et al. [13].

ALD was also used to deposit the chromia precursor (chromium acetyl acetonate, $Cr(acac)_3$, Riedel-de Haën 99%) on the zirconia, alumina, and zirconia/alumina supports. The chromia deposition technique is similar to the technique used for zirconia deposition [7]. After the $Cr(acac)_3$ deposition the surface acac complexes were decomposed to form the chromium oxide by using air at elevated temperature. Two sequences of complex formation and decomposition were used to prepare chromia catalysts containing 1–2 $at_{Cr}/nm^2$. The catalysts were calcined in air at 600 °C for 4 h.

The surface area and porosity of the catalysts were determined by the BET method [17]. The amounts of chromium and zirconium were determined by X-ray fluorescence (XRF). X-ray photoelectron spectroscopy (XPS) was used to study the surface composition of the calcined catalysts [17]. The amount of $Cr^{6+}$ on the calcined catalysts was analyzed by UV–vis spectrophotometry (UV-Shimadzu, λ = 375 nm) after dissolution of $Cr^{6+}$ by aqueous sodium hydroxide. The method is described in detail by Haukka [20].

### 2.2. Isobutane dehydrogenation activity measurements

The isobutane dehydrogenation activities of the catalysts were measured in a continuous flow reaction system consisting of a fixed-bed microreactor, and a Fourier transform infrared (FTIR) gas analyzer and a gas chromatograph (GC) for on-line product analysis. All gases were from AGA (synthetic air 99.99%, nitrogen 99.999%, isobutane 99.95%, and hydrogen 99.999%). Nitrogen was further purified with Oxisorb (Messer Griesheim GmbH).

The activity measurements were carried out at 560 °C under atmospheric pressure. The samples (0.1 g) were loaded in the reactor between two layers of silicon carbide (SiC) and were heated to the reaction temperature under 5% $O_2/N_2$. Dehydrogenation was carried out for 15 min using isobutane feed with a weight hourly space velocity (WHSV) of 15 $h^{-1}$ and diluted with nitrogen at a molar ratio of 3:7. The reaction products were monitored by FTIR for the first 6 min on stream, a GC sample was taken after 10 min, and the FTIR analysis was continued after this. After the dehydrogenation, the catalyst was regenerated with diluted air. The regeneration products – carbon oxides and water – were analyzed by FTIR. The amount of coke (as carbon) deposited on the catalyst during dehydrogenation was calculated from the measured amounts of carbon oxides. The amount of water formed was indicative of the amount of hydrogen in the coke. In selected experiments the catalyst was prereduced with 10% $H_2/N_2$ for 15 min before the dehydrogenation. Water formed in the prereduction was analyzed by FTIR. Thermal reactions in the system were investigated by replacing the catalyst with inert SiC.

The gaseous products were analyzed on-line with a Gasmet FTIR gas analyzer (Gasmet Technologies) equipped with a Peltier-cooled mercury–cadmium–telluride detector, and with an HP 6890 gas chromatograph equipped with an HP PLOT/$Al_2O_3$ "M" column and a flame ionization detector. The FTIR spectra were recorded in the wavenumber range 4000–850 $cm^{-1}$ with a resolution of 8 $cm^{-1}$ and a scanning rate of 10 scans/s. The analysis cuvette (9 $cm^3$) was kept at constant temperature (180 °C) and pressure (103 kPa). The spectra were measured every 2 s during the first 2 min on stream, every 5 s during the next 2 min, and thereafter every 30 or 60 s. Further details of the FTIR gas analysis method, and of the determination of the product distribution based on the measured spectra can be found elsewhere [21,22]. The conversions, selectivities, and yields were calculated on a molar basis as presented in [21].

### 2.3. In situ DRIFTS

In situ DRIFTS was used to characterize the calcined catalysts and to study the formation of surface species during isobutane dehydrogenation. The equipment consisted of a Nicolet Nexus FTIR spectrometer equipped with a Spectra-Tech high temperature and high pressure reaction chamber (ZnSe windows). A Pfeiffer Vacuums Omnistar mass spectrometer (MS) was used to monitor the gaseous products on-line. All samples were studied undiluted in powder form and calcined in situ with 10% $O_2/N_2$ at 580 °C for 2 h. In all experiments the spectrum measured with an aluminum mirror (4 $cm^{-1}$, 200 scans) was used as the background, and the total gas flow was kept constant at 50 $cm^3$/min. All gases were from AGA (synthetic air 99.99%, $N_2$ 99.999%, isobutane 99.95%, and $H_2$ 99.999%). Nitrogen was further purified with Oxisorb (Messer Griesheim GmbH).

The performance of the catalysts in dehydrogenation of isobutane was studied with two different approaches. The experiments were performed either as (i) temperature-dependent, where the catalysts were heated slowly in 5% isobutane in nitrogen from room temperature to 580 °C, or as (ii) time-dependent studies, where the dehydrogenation performance of the catalysts was studied at the constant temperature of 580 °C under 5% isobutane in nitrogen. During the temperature-dependent measurement the spectra were first

recorded at 30, 50, 75, and 100 °C (4 $cm^{-1}$, 100 scans), after which the sample was flushed with nitrogen for 5 min at 100 °C. After the flush, a spectrum (4 $cm^{-1}$, 100 scans) was recorded under nitrogen at 100 °C. The experiment was continued by redirecting the isobutane flow to the sample and by heating slowly. The spectra were recorded every 25 °C under isobutane and at 100, 200, 300, 400, 500, and 580 °C under nitrogen. During the time-dependent measurements at 580 °C the dehydrogenation performance was studied by feeding isobutane for 3, 3, 4, 5, 5, and 10 min (total 30 min) to the sample with 5 min nitrogen flushes in between the isobutane sequences. Spectra were recorded every minute (4 $cm^{-1}$, 30 scans). The samples were reoxidized at 580 °C after the experiments with 2–10% $O_2/N_2$ for 30 min.

The effect of hydrogen prereduction (5% $H_2/N_2$) was studied with both temperature- and time-dependent measurements. The prereduction was done at 580 °C for 15 min during which spectra were recorded every minute (4 $cm^{-1}$, 30 scans) for the first 8 min on stream and then once after 9 and 12 min (4 $cm^{-1}$, 100 scans). After the prereduction the sample was either flushed with nitrogen for 10 min at 580 °C after which it was cooled to room temperature under nitrogen followed by the temperature-dependent isobutane experiment, or it was flushed with nitrogen for 30 min at 580 °C followed by the time-dependent measurement.

### 2.4. In situ Raman spectroscopy

The in situ Raman–MS measurements were performed to study the chromium and hydrocarbon surface species formed during dehydrogenation on the chromia catalysts at the constant temperature of 570 °C. The measurements were performed with a Renishaw Micro-Raman System-1000 using a home-made quartz flow-through reactor (operando reactor [23]) and a MS for on-line product analysis. The Raman spectrometer consisted of an $Ar^+$ (514 nm) laser, a cooled CCD detector, and a holographic super-Notch filter for the removal of elastic scattering. The catalyst sample was loaded to the reactor between two layers of silicon carbide to minimize the void volume inside the reactor. The catalyst samples were calcined using 5% $O_2$/He at 570 °C for 2 h after which the reactor was flushed with helium for 30 min before the experiments. The dehydrogenation measurements were performed at 570 °C by feeding 5% isobutane in nitrogen to the sample. The spectra were recorded after 2, 12, 22, and 32 min on stream under isobutane. The acquisition of one spectrum required 9 min. After the dehydrogenation, the samples were flushed with helium for 30 min and reoxidized using 5% $O_2$/He for 30 min.

## 3. Results

### 3.1. Characterization of the catalysts

Table 1 presents the surface areas and elemental composition of the samples measured by BET and XRF, respectively [17]. The characterization and surface composition of the zirconia-, alumina-, and zirconia/alumina-supported chromia catalysts has been reported in detail elsewhere [17]. Therefore, only a short summary will be given here. The zirconia/alumina supports had a zirconium surface density either below, or approximately equal to the monolayer coverage of ~4 $at_{Zr}/nm^2$. Their surface area was in the same order of magnitude as that of alumina, whereas the surface area of pure zirconia was one-third of that. No crystalline zirconia was observed by Raman spectroscopy for the zirconia/alumina supports, whereas the pure zirconia was mainly monoclinic. No indication of the formation of a mixed oxide was observed by XPS [17]. Methanol adsorption–desorption experiments suggested a strong interaction between zirconia and alumina for these supports [17].

The hydroxyl groups for the zirconia/alumina support resembled more those of alumina than those of zirconia. Damyanova et al. [10] and Kytökivi et al. [13] also reported that the hydroxyls for zirconia/alumina did not resemble those of zirconia even at zirconia loadings near the monolayer coverage. Pyridine adsorption measurements on zirconia/alumina have shown that the deposition of zirconia reduces the concentration of strong Lewis acidic sites, whereas the concentration of weak Lewis acidic sites increases [10]. In our methanol adsorption–desorption measurements [17], where the formation of dimethylether (DME) was indicative of surface Lewis acid species, the strength of Lewis acidity was highest for pure alumina. The deposition of zirconia on alumina decreased the Lewis acidity of the support. DME was not formed on pure zirconia.

The chromium surface density for the catalysts was 1–2 $at_{Cr}/nm^2$, which is below the monolayer coverage of ~4–5 $at_{Cr}/nm^2$. No crystalline $\alpha$-$Cr_2O_3$ was observed for the catalysts by Raman spectroscopy [17]. The Raman spectroscopic measurements showed that the chromates for the calcined catalysts were polychromates [17]. Table 1 presents the UV–vis results on the amount of $Cr^{6+}$ species for the calcined catalysts. In agreement with our earlier XPS results [17], a higher fraction of chromium was in the oxidation state +6 than in the oxidation state +3 on the calcined catalysts. However, the UV–vis measurement technique for the quantification of $Cr^{6+}$ species is more accurate for the chromia/alumina catalyst than for the chromia/zirconia catalyst due to the higher fraction of $Cr^{5+}$ species present on the zirconia support. $Cr^{5+}$ species are not stable in aqueous solutions and tend to disproportionate ($3Cr^{5+} \rightarrow 2Cr^{6+} + Cr^{3+}$) into soluble $Cr^{6+}$ and finely dispersed, surface bound $Cr^{3+}$ hydroxide [9]. It is suggested that the oxidation state distribution of the chromia species on zirconia/alumina resembled more that of the alumina-supported catalyst than the zirconia-supported one.

### 3.2. Activity measurements

Isobutane dehydrogenation activities were measured for the chromia catalysts described in Table 1, and for the 4.4ZrAl, alumina, and zirconia supports. Fig. 1 shows the yields of isobutene and cracking products ($C_1$–$C_3$ hydrocarbons) obtained with the supports and in thermal reactions investigated with inert silicon carbide. No reduction products (carbon oxides

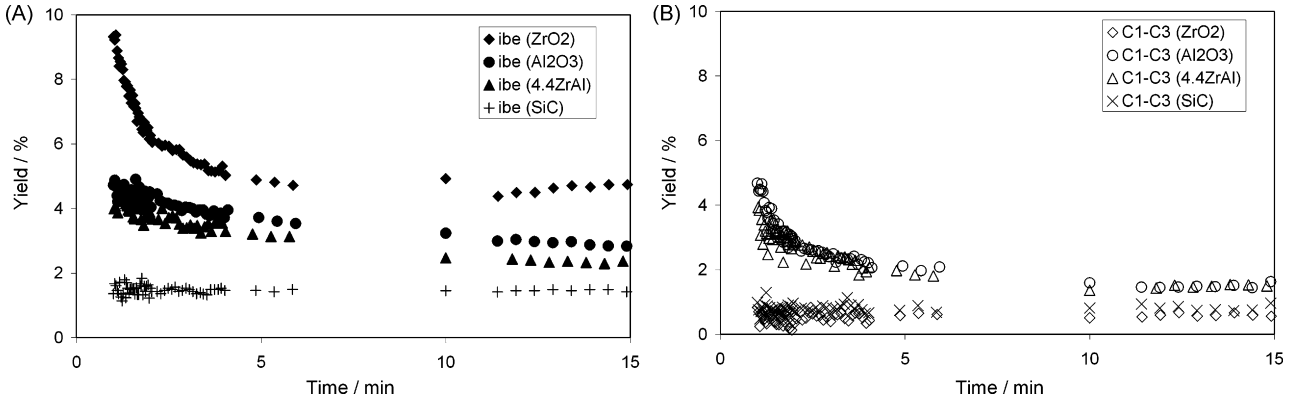


Fig. 1. (A) Yields of isobutene (ibe, solid symbols) and (B) $C_1$–$C_3$ hydrocarbons (cracking products, open symbols) in isobutane dehydrogenation for the 4.4ZrAl, alumina, and zirconia supports.

or water) were released from the supports. The dehydrogenation and cracking activities were similar for the 4.4ZrAl and alumina supports, whereas the zirconia support had a higher dehydrogenation activity but the cracking products were mainly formed in thermal reactions.

The isobutane dehydrogenation activities of the supported chromia catalysts were measured after calcination and after prereduction by hydrogen. The calcined catalysts were reduced during the first minute(s) on isobutane stream or on hydrogen stream seen as a release of carbon oxides or water, respectively. Based on the amount of the reduction products and the amount of $Cr^{6+}$ on the calcined catalysts, the average oxidation state of chromium for the 2.1(15)CrZrAl and the 2.2CrAl was +3 after the reductions. For the 0.8CrZr catalyst this calculation was not accurate due to the uncertainty in the amount of $Cr^{6+}$ and $Cr^{5+}$ for the calcined catalyst. Fig. 2 shows the yield of isobutene obtained during dehydrogenation. After calcination, the two chromia/zirconia/alumina catalysts had lower dehydrogenation activities than the 0.8CrZr and 2.2CrAl catalysts had. The yields of cracking products were the same with a catalyst or with inert silicon carbide, indicating that cracking was mainly a thermal reaction. The yield of cracking products for the 2.0(4.4)CrZrAl catalyst was slightly higher than for the other chromia catalysts, but the difference was not significant. Prereduction of the catalysts by hydrogen decreased the dehydrogenation activities, the decrease being the most apparent for the alumina- and zirconia/alumina-supported samples.

Fig. 3 summarizes the dehydrogenation activities of the calcined supports and catalysts and the coke contents after dehydrogenation. The isobutene yields were measured at 2 min on stream, at which time the catalysts were reduced but had not yet severely deactivated. The yields of cracking products were calculated as an average over 10 measurement points between 2 and 3 min on isobutane stream. The coke content after dehydrogenation was lower on the 4.4ZrAl support than on the alumina support, although their activities were similar. The coke content was low also on the zirconia support, even though it had the highest dehydrogenation activity. On the contrary, for the chromia catalysts the coke content was lower on the alumina- and zirconia/alumina-supported catalysts than on the 0.8CrZr catalyst. In addition, the hydrogen content for the coke on the 0.8CrZr catalyst was lower than for the alumina-containing catalysts; the approximate H/C ratios were 0.2, 0.6, and 0.8 for the 0.8CrZr, 2.1(15)CrZrAl, and 2.2CrAl catalysts, respectively (not shown). For the prereduced catalysts the amount of coke deposited decreased in accordance with the decreased activity.

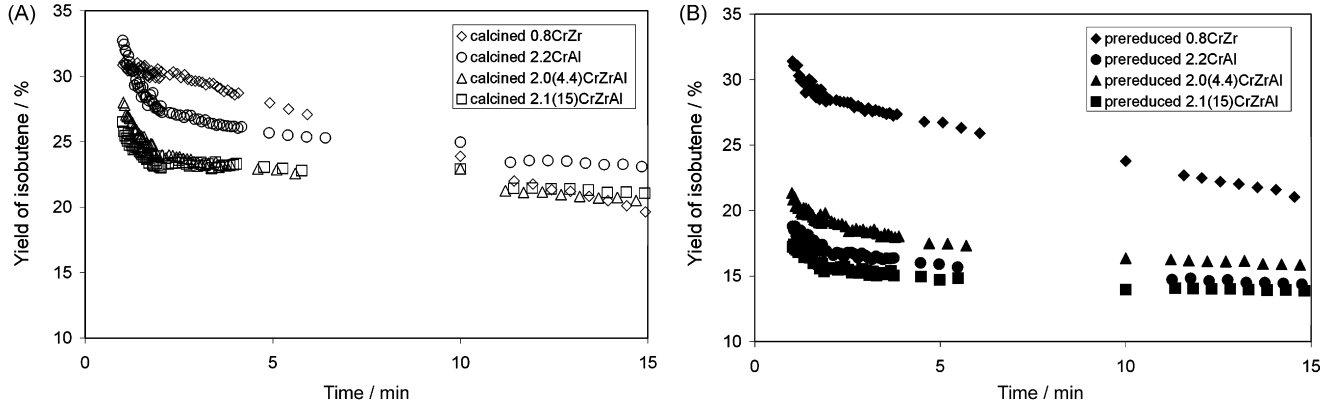


Fig. 2. Yield of isobutene in isobutane dehydrogenation for (A) the calcined (open symbols) and (B) hydrogen prereduced (solid symbols) chromia catalysts.

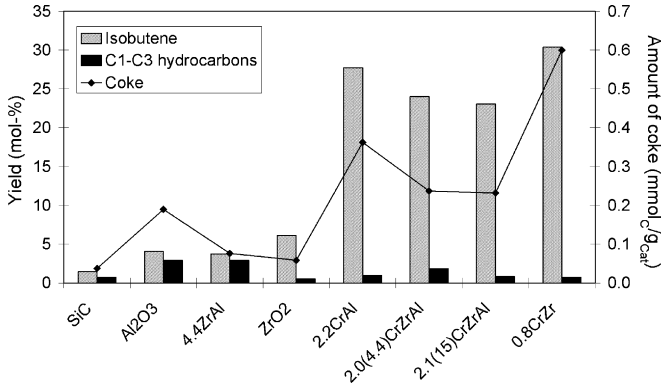


Fig. 3. Summary of the performance of the supports and chromia catalysts during the dehydrogenation. The grey and the black columns present the yields (left axis) of isobutene and cracking products ($C_1$–$C_3$ hydrocarbons), respectively. The isobutene yields are at 2 min on stream and the yields for the cracking products are an average of observed amounts between 2 and 3 min on stream. (◆) Presents the amount of coke (as carbon) formed during the dehydrogenation (right axis). The connecting line has been added to guide the eye.

### 3.3. In situ DRIFTS

#### 3.3.1. Temperature-dependent measurements

The temperature-dependent measurements were performed for all chromia catalysts, and for the 4.4ZrAl, zirconia, and alumina supports to study the formation and stability of the different carbonaceous surface species on the catalysts, and their relevance to the dehydrogenation. Fig. 4 presents as an example spectra measured for the 2.0(4.4)CrZrAl catalyst during the temperature-dependent measurement. The spectra were recorded during nitrogen flushes to increase the observability of the bands of the surface species in the C–H stretching region.

Table 2 presents a summary of the observed bands and their assignments for the catalysts. The strong band at 2340 $cm^{-1}$ observed for all of the samples is assigned to carbon dioxide impurities inside the support [24]. For the zirconia/alumina- and alumina-supported catalysts the formation of water (~1630 $cm^{-1}$) and acetone (~1680 ($\nu$(CO) and 1248 $cm^{-1}$ [25])) was less pronounced than for the zirconia-supported catalyst. At 100 °C also a band at ~2980 $cm^{-1}$ was observed for all catalysts. This band is tentatively assigned to a $\nu(CH_3)$ vibration of a *tert*-butoxide species [26]. Starting from 200 °C the formation of formates was observed for all catalysts from the bands around 2975 ($\nu_{as}$(COO) + $\nu_s$(COO)), 2880 ($\nu$(CH)), 2750 ($\nu_s$(COO) + $\delta$(CH)), 1562 ($\nu_{as}$(COO)), 1380 ($\delta$(CH)), 1365 ($\nu_s$(COO)), and 1350 $cm^{-1}$ [25,27,28]. The formate bands reached their maximum intensities around 400 °C. Around 325 °C the chromates were observed to reduce as the $Cr^{6+}$ = O [4] bands at ~2000 $cm^{-1}$ disappeared from the spectra. Simultaneously with the decrease in the intensity of the bands of the formate species, bands assigned to carboxylate-type species, also assigned to acetates by Finocchio et al. [27], were observed at ~1530 ($\nu_{as}$(COO)), ~1430 ($\nu_s$(COO)), and ~1350 $cm^{-1}$.

Approximately at 400 °C bands assigned to adsorbed isobutene [29] (3103, 1638, 1472, and 1239 $cm^{-1}$) were observed for the 0.8CrZr catalyst. Bands at 3102 $cm^{-1}$, and at 3106 and 1242 $cm^{-1}$ were also observed for the 2.0(4.4)CrZrAl and the 2.1(15)CrZrAl catalysts, respectively. However, these were lower in intensity and appeared at slightly higher temperature than for the 0.8CrZr catalyst. The formation of dehydrogenation products (hydrogen and isobutene) was observed by MS approximately at the same temperature as the bands of adsorbed isobutene and, therefore, the appearance of adsorbed isobutene can be linked with the start of the dehydrogenation reaction.

At the highest temperature studied (580 °C) bands of the carboxylate-type species and of aliphatic [30,31] (~2980 and ~2940 $cm^{-1}$) and unsaturated/aromatic [26,30] (~3060 $cm^{-1}$) hydrocarbons were observed for the alumina-containing catalysts. The band at ~2940 $cm^{-1}$ is assigned to a $\nu_{as}$(CH) vibration of a methylene-type (>$CH_2$) group, whereas the band

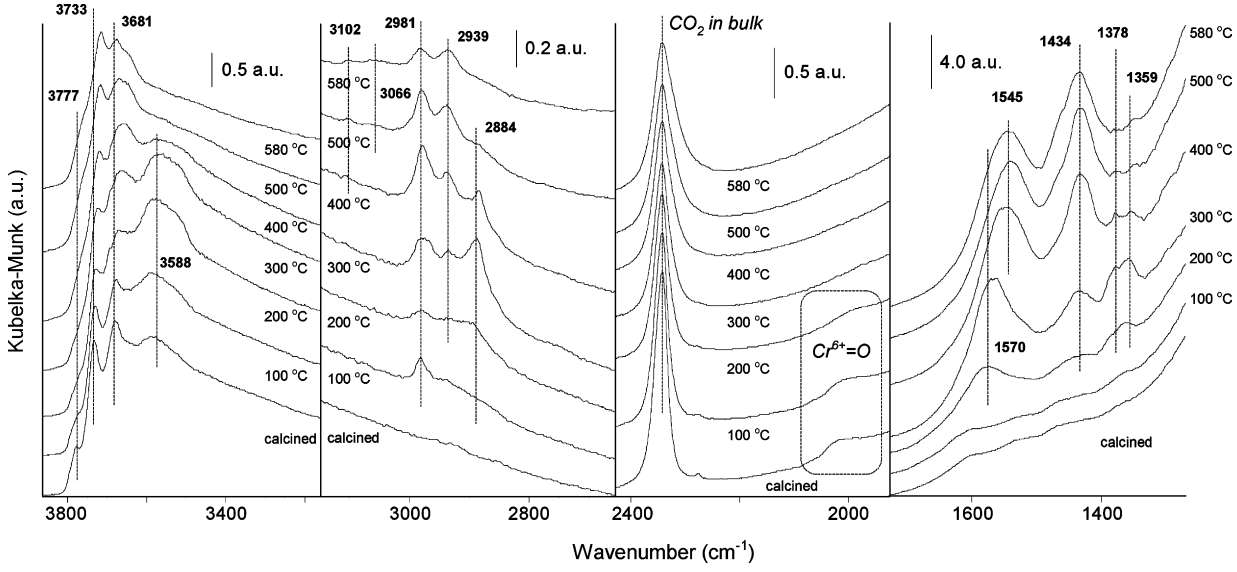


Fig. 4. In situ DRIFT spectra for temperature-dependent dehydrogenation for the 2.0(4.4)CrZrAl. Spectra recorded during nitrogen flushes.

Table 2
The observed in situ DRIFTS bands and their assignments in the temperature-dependent measurements

| Sample | *tert*-Butoxide [26] | Water | Acetone [25] | Formate [25,27,28] | Carboxylate | ibe[a] [29] | Aliphatic [30,31] | Unsaturated/ aromatic [26,30] |
|---|---|---|---|---|---|---|---|---|
| 0.8CrZr | 2977 | 1623 | 1673, 1242 | 2972, 2885, 2745, 1568, 1378 (sh)[b], 1366, 1350 | 1530, 1430, 1350 | 3103, 1636, 1238 | 2979, 2929 | 3062 |
| 2.2CrAl | 2983 | 1630 (sh)[b] | 1675 (sh)[b] 1245 (w)[c] | 2976, 2885, 2742 (w)[c], 1565, 1379 (sh)[b], 1363 | 1541, 1435 | n.o.[d] | 2981, 2935 | 3053 |
| 2.0(4.4)CrZrAl | 2981 | n.o.[d] | n.o.[d] | 2975, 2884, 2745 (w)[c], 1570, 1378 (sh)[b], 1359 | 1545, 1434 | 3102 | 2980, 2939 | 3066 |
| 2.1(15)CrZrAl | 2981 | 1632 | 1681 | 2975, 2887, 2746, 1567, 1380 (sh)[b], 1367 | 1543, 1438, 1348 | 3106, 1224 | 2978, 2938 | 3053 |

[a] ibe: isobutene.
[b] sh: shoulder.
[c] w: weak.
[d] n.o.: not observed.

at ~2980 $cm^{-1}$ could originate from a $\nu_{as}$(CH) vibration of a methyl-type (–$CH_3$) group. The band at ~2980 $cm^{-1}$ disappeared from the spectra of the 0.8CrZr catalyst above 500 °C, after which the carboxylate-type and unsaturated/aromatic species, and a methylene-type vibration were observed.

The temperature-dependent measurements were also done after hydrogen prereduction. Fig. 5 presents as an example spectra measured for the prereduced 2.0(4.4)CrZrAl sample. The spectra were recorded under nitrogen as described earlier. After prereduction the formation of water, acetone, and formates was suppressed. This suggests that the formation of these species required interaction of the gas phase with the $Cr^{6+}$ species, or that the hydrogen prereduction was able to suppress their formation, e.g. by inhibiting the adsorption of isobutane at low temperatures. At 100 °C the only band arising from the surface bound carbonaceous species for all catalysts was observed at ~2980 $cm^{-1}$, and was assigned to *tert*-butoxide as discussed previously. This band was lower in intensity for the prereduced catalysts than for the calcined ones. For the alumina-containing catalysts this band disappeared with heating and no bands of carbonaceous surface species were observed at 200 °C. For the 0.8CrZr at 200 °C low intensity bands assigned to the carboxylate-type species were observed. For the alumina-containing catalysts these species were observed starting at approximately 300 °C.

Approximately at 300 °C low intensity bands assigned to the formates were observed for the 0.8CrZr at ~2880, ~1570, and ~1370 $cm^{-1}$, but these bands were only observable up to 400 °C. For the 0.8CrZr catalyst the bands of adsorbed isobutene were observed as during the experiment for the calcined sample. For the zirconia/alumina- and alumina-supported catalysts these bands were not observed. At the highest temperature studied (580 °C) the bands assigned to the aliphatic and carboxylate-type species were observed at ~2980, ~2940, and at ~1530, ~1430 $cm^{-1}$, respectively, for the zirconia/alumina- and alumina-supported catalysts, whereas for the zirconia-supported catalyst the formation of unsaturated/aromatic species (3060 $cm^{-1}$) was observed in addition to the

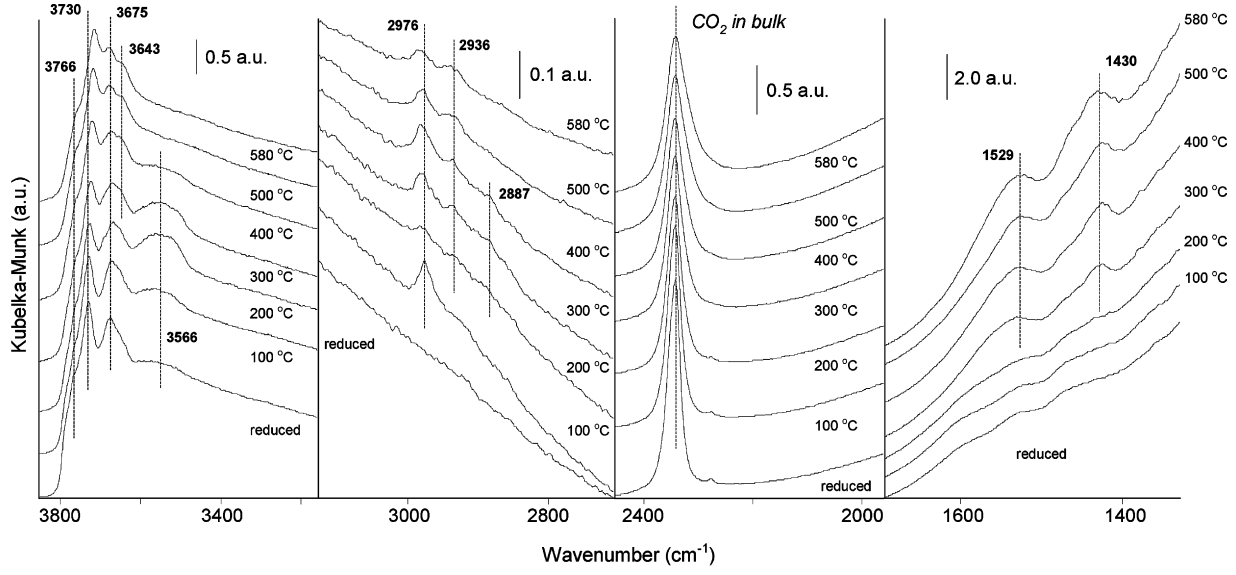


Fig. 5. In situ DRIFT spectra for temperature-dependent dehydrogenation for the hydrogen prereduced 2.0(4.4)CrZrAl. Spectra recorded during nitrogen flushes.

bands of the carboxylate-type and aliphatic species. In accordance with the experiment for the calcined 0.8CrZr the band at ~2980 $cm^{-1}$ was only observable up to 500 °C. The prereduction seems to suppress the formation of all carbonaceous surface species for the zirconia/alumina- and alumina-supported catalysts, whereas for the zirconia-supported one only the formation of acetone, water, and formates was affected.

### 3.3.2. Time-dependent measurements

The time-dependent measurements were performed for all chromia-containing catalysts and for all supports to study the formation of carbonaceous surface species at high temperature and their effect on the activity of the catalysts as a function of reaction time. Fig. 6 presents a comparison of the bands in the C–H stretching region. The spectra were recorded during nitrogen flushes. For all calcined catalysts the formation of the carboxylate-type and aliphatic species was observed after short time on isobutane stream, whereas the formation of the unsaturated/aromatic species required a longer time. The performance of the zirconia/alumina-supported catalysts resembled that of the alumina-supported one rather than that of the zirconia-supported catalyst. After the first isobutane feed (3 min) aliphatic surface species were observed for all catalysts. For the 0.8CrZr catalyst, however, only the band at 2927 $cm^{-1}$ (methylene-type) was observed, whereas for the alumina-containing catalysts bands at ~2980 (methyl-type) and ~2940 $cm^{-1}$ (methylene-type) were observed. With time on stream the band at ~2980 $cm^{-1}$ decreased in intensity for the alumina-containing catalysts. The methyl band at ~2980 $cm^{-1}$ was more intense for the 2.2CrAl catalyst than for the other catalysts after 30 min of dehydrogenation. This order is in accordance with that observed for the H/C ratios of coke in the activity measurements. Therefore, the band may correlate with the hydrogen content of the coke. For the alumina-containing catalysts also a low intensity band at ~3104 $cm^{-1}$ was observed possibly originating from adsorbed isobutene. After 6 min on isobutane stream the formation of the band at ~3060 $cm^{-1}$, assigned to the unsaturated/aromatic species, was observed for all catalysts. The band increased in intensity with time on stream with a decrease in the amount of isobutene and hydrogen in the product stream (MS) suggesting that the catalysts deactivated due to coke formation.

Fig. 7 presents a similar comparison as presented in Fig. 6 for the hydrogen prereduced catalysts. Similar to the temperature-dependent experiments, the formation of carbonaceous surface species was suppressed for the alumina-containing catalysts, whereas the 0.8CrZr was affected only little. For the 0.8CrZr bands originating from the vibrations of unsaturated/aromatic surface species (3064 $cm^{-1}$) and methylene-type groups (2928 $cm^{-1}$) were observed. The 3064 $cm^{-1}$ band increased in intensity with time on stream with a decrease in the amount of dehydrogenation products. For the alumina-containing catalysts no bands of adsorbed isobutene or unsaturated/aromatic species could be observed, and those arising from the carboxylate-type and aliphatic surface species were low in intensity.

### 3.4. In situ Raman–MS measurements

The in situ Raman–MS measurements were performed for the zirconia-, alumina-, and zirconia/alumina-supported chromia catalysts to further study the formation of the carbonaceous surface species under isobutane at high temperature. In accordance with the activity measurements the MS measurements showed that the catalysts deactivated with time on stream

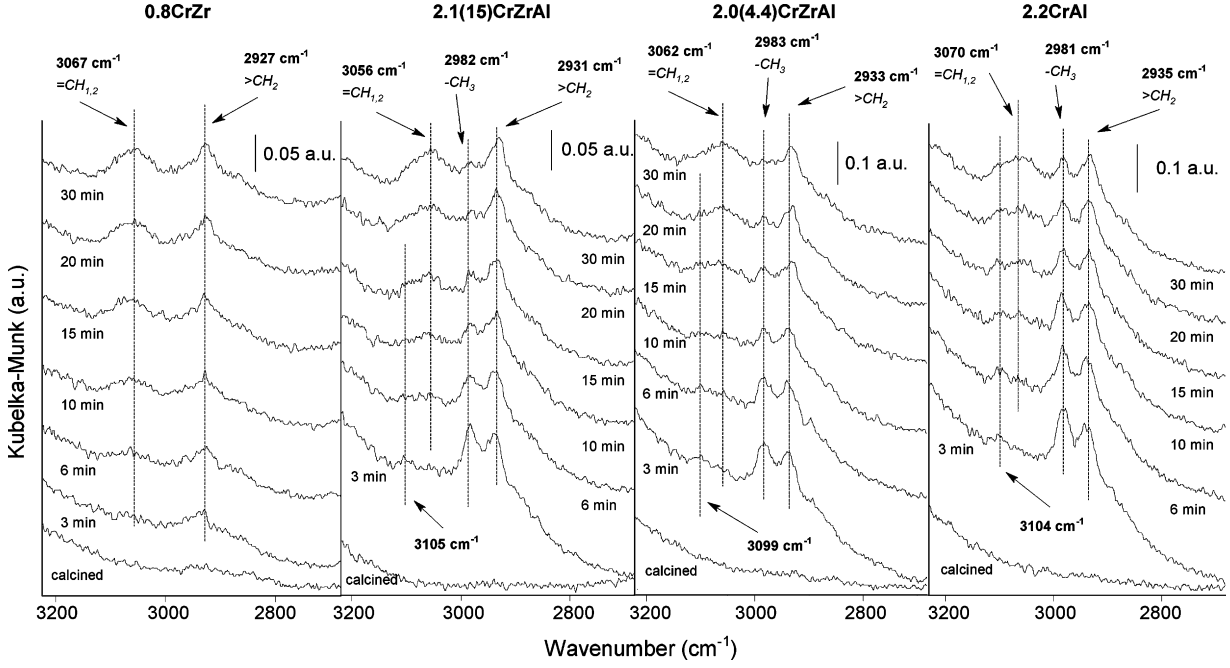


Fig. 6. Comparison of the bands observed by in situ DRIFTS in the C–H stretching region during time-dependent dehydrogenation at 580 °C for the calcined catalysts. Spectra recorded during nitrogen flushes.

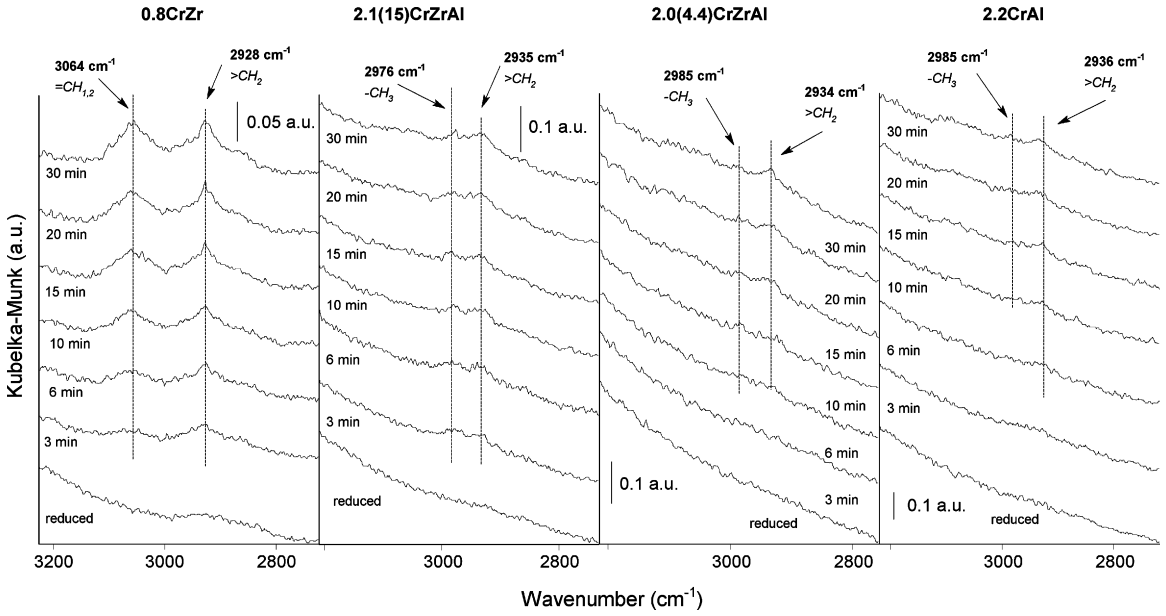


Fig. 7. Comparison of the bands observed by in situ DRIFTS in the C–H stretching region during time-dependent dehydrogenation at 580 °C for the hydrogen prereduced catalysts. Spectra recorded during nitrogen flushes.

(not shown). Fig. 8 presents the Raman spectra recorded for the 2.1(15)CrZrAl and 0.8CrZr catalysts under isobutane at 570 °C. The spectrum of the quartz window has been subtracted from the spectra. For the alumina-supported catalyst no spectra could be obtained due to intense fluorescence under the dehydrogenation conditions in accordance with Weckhuysen and Wachs [32]. In accordance with the in situ DRIFTS measurements the chromates reduced immediately after the start of the isobutane feed. Carbonaceous surface species were observed for both zirconia- and zirconia/alumina-supported catalysts at ∼1585 and ∼1339 $cm^{-1}$. These bands were assigned to pregraphitic deposits (coke) in accordance with Kuba and Knözinger [33]. Additional bands with lower intensities were also observed at ∼2880 $cm^{-1}$ (not shown), assigned to C–H vibrations of the carbonaceous species [34]. The bands were formed for the 0.8CrZr already after 2 min on stream, whereas for the 2.1(15)CrZrAl their formation required a longer time. For alumina-supported chromia catalysts with high chromium loadings similar bands have been observed during propane dehydrogenation, but only after 20 min on stream [34]. With increasing time on stream the bands of monoclinic zirconia disappeared from the spectra for the 0.8CrZr. A similar behavior was also observed by Kuba and Knözinger [33] for sulfated- and tungstated-zirconia catalysts in the isomerization of *n*-pentane, and was assigned to the darkening of the sample due to coke formation.

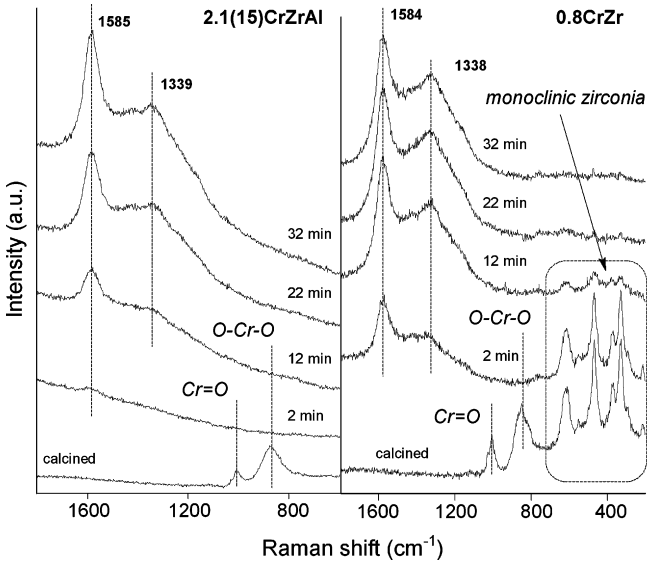


Fig. 8. In situ Raman spectra for the 2.1(15)CrZrAl and 0.8CrZr catalysts under dehydrogenation conditions. The spectrum of the quartz window has been subtracted from all spectra.

## 4. Discussion

The dehydrogenation reaction and the formation of carbonaceous surface species on the zirconia/alumina-, alumina-, and zirconia-supported chromia catalysts were studied by activity and by in situ DRIFTS and in situ Raman spectroscopic measurements.

The zirconia/alumina and alumina supports were slightly active in dehydrogenation and cracking of isobutane, whereas the zirconia support was active in dehydrogenation only. The amount of coke formed was highest for the alumina, somewhat lower for the 4.4ZrAl support, and lowest for the zirconia. This can be compared with the methanol adsorption–desorption results on the Lewis acidic properties of the supports. Our methanol adsorption–desorption measurements [17] indicated that alumina had the highest Lewis acidity, i.e. the lowest temperature for the formation of dimethylether (DME). The deposition of both chromia and zirconia on the alumina decreased the Lewis acidity, i.e. increased the temperature of

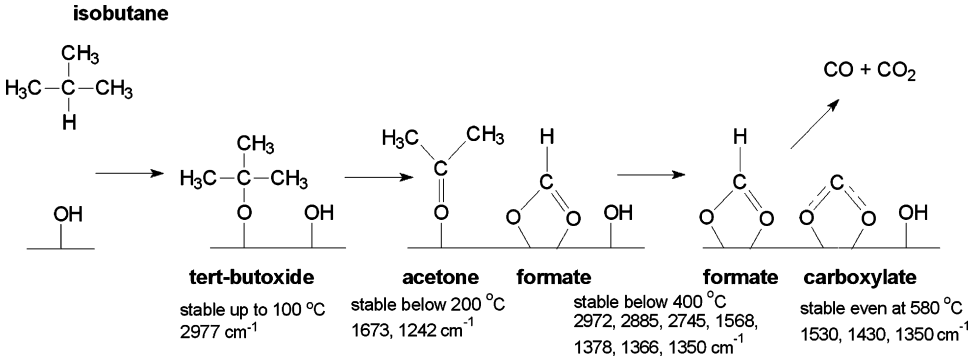


Fig. 9. The suggested reaction mechanism for the formation of the oxygenated carbonaceous species. The mechanism has been adapted from the results by Ermini et al. [35] and Finocchio et al. [25,27]. The in situ DRIFTS bands observed for the 0.8CrZr are presented for each species.

DME formation. No DME was formed for the pure zirconia support or for the 0.8CrZr catalyst. Therefore, the amount of coke on the different supports followed the order of Lewis acidity of the support materials rather than the order of dehydrogenation activity. Furthermore, the higher cracking activity can be assigned to the Lewis acidity of the alumina and the zirconia/alumina.

The in situ DRIFTS temperature-dependent studies showed similarities between all studied catalysts. The main reason for the similar behavior is that the observed oxygenated species are mainly spectators that are formed during the reduction of the $Cr^{5+}/Cr^{6+}$ species. Fig. 9 presents a summary of the formation of the different oxygenated species from isobutane for the calcined catalysts during the temperature-dependent measurements. The scheme has been adapted from the results presented by Finocchio et al. [25,27] and Ermini et al. [35]. Similar results have also been reported for the interactions of propane [34] and isobutane [36] on chromia/alumina catalysts with a high chromium loading. The main route for the formation of the oxygenated species, i.e. acetone, formate, and carboxylate-type species, is due to the reduction of the $Cr^{5+}/Cr^{6+}$ species. However, Ermini et al. [35] also observed that the Brønsted acidic hydroxyl groups of pure alumina were able to convert propane into the oxygenated species. In our experiments the monoclinic zirconia was the most active support both in the formation of oxygenated surface species and in the dehydrogenation reaction. Since no reaction products of the basic or Lewis acidic surface sites were observed for zirconia in our earlier methanol adsorption–desorption experiments [17], the Brønsted acidic hydroxyl groups or the acid-base pair ($Zr^{4+}$–$O^{2-}$) would seem likely sites for the reactivity of zirconia. However, the observed oxygenated carbonaceous surface species are not directly related to the formation of the dehydrogenation reaction products but are spectators.

On the prereduced catalysts the formation of water, acetone, and formates were suppressed mainly due to the absence of $Cr^{5+}/Cr^{6+}$ species. However, some formates were observed for the 0.8CrZr, but their formation required higher temperatures suggesting that these species were formed for the prereduced catalysts as the support reacted with the isobutane feed. The hydrogen prereduction also suppressed the formation of the other carbonaceous surface species (aliphatic and unsaturated/aromatic) for the alumina-containing catalysts. In addition, the activity measurements showed that the dehydrogenation activity of these catalysts was lower after the prereduction. The results suggest that, especially, for the alumina-containing supports, hydrogen prereduction was able to inhibit the formation of both the surface species and the dehydrogenation products. The inhibition might originate from the formation of higher concentrations of surface bound water on the alumina-containing catalysts [21], although it is not possible to conclude this from the DRIFTS results.

The 0.8CrZr was the most active catalyst in the dehydrogenation of isobutane even though it had the lowest chromium content in weight percentage. The zirconia deposition on alumina decreased the dehydrogenation activity since the 2.2CrAl catalyst was more active than the two chromia/zirconia/alumina catalysts. On the contrary, Gaspar and Dieguez [15] reported a slightly higher dehydrogenation activity, reported in TON (turn over number), for their chromia/zirconia/alumina catalyst – containing a low surface density of zirconia and no XRD observable zirconia crystallites similar to our zirconia/alumina supports – compared with that for their chromia/alumina catalyst. However, they did not speculate on the reasons for the higher activity, and the characterization results they reported do not allow this to be done here. In agreement with our results, Burch and Loader [18] found the use of zirconia/alumina as the support to decrease the activity of their rhodium catalysts in the combustion of methane and in the reduction of nitrogen oxide compared with the use of zirconia or alumina, respectively, as the support. They suspected that an incomplete monolayer of zirconia on alumina caused rhodium to interact with both oxides instead of just with zirconia modifying the active species. This incomplete coverage of alumina by zirconia could also be true with our catalysts.

Our results suggested that the support Lewis acidity increased the cracking activity and the coke deposition rate for the bare supports. For the chromia catalysts this effect was not apparent because the formation of cracking products was mainly a thermal reaction and did not depend on the catalyst. The amount of deposited coke, on the other hand seemed to depend on the dehydrogenation activity suggesting that coke was formed from adsorbed isobutene. Similar results have been

reported for the dehydrogenation of propane on vanadia/alumina catalysts [37]. Infrared bands assigned to adsorbed isobutene were observed for all zirconia-containing chromia catalysts. These bands were observed at slightly lower temperatures for the chromia/zirconia than for the chromia/zirconia/alumina suggesting that the dehydrogenation reaction occurred more readily on the chromia/zirconia catalyst. In accordance with the activity results the higher coke deposition rate for the 0.8CrZr catalyst was observed by in situ DRIFTS and in situ Raman spectroscopy.

The higher activity of chromia/zirconia compared with the activities of the alumina- and zirconia/alumina-supported chromia catalysts might originate from more easily available chromium species or from a beneficial interaction between the zirconia support and the chromium species. However, the activity of the chromia catalysts is not governed by the acidity of the material only, but the phase of the zirconia seems important as well, and this may account for differences with previous literature reports [15]. A higher zirconia loading on alumina, exceeding the monolayer, might increase the dehydrogenation activity of the zirconia/alumina-supported chromia catalyst. However, the surface area of the support decreases (see Table 1) with increasing zirconia loading gradually canceling the beneficial effect on the surface area. In addition the formation of zirconia crystallites may lead to an inhomogeneous surface, where both alumina and zirconia are able to interact with the chromium species. Therefore, the deposition of zirconia on alumina does not seem to be the solution (i) to increase the activity of chromia/alumina catalysts in the dehydrogenation, or (ii) to increase the surface area of chromia/zirconia catalysts. Nevertheless, the rate of coke deposition decreased for the pure supports suggesting that the deposition of zirconia on alumina might be beneficial for applications where the support acidity has a more direct influence on the performance of the catalyst.

## 5. Conclusions

The effect of zirconia deposition on alumina was studied for chromia dehydrogenation catalysts by activity measurements and by in situ DRIFT and in situ Raman spectroscopic measurements. The results were compared with the performance of chromia/zirconia and chromia/alumina catalysts all containing chromium below 2 $at_{Cr}/nm^2$. The in situ DRIFTS measurements revealed the formation of spectator species (acetone, formates, and carboxylate-type species) and coke (aliphatic and unsaturated/aromatic hydrocarbon species) from isobutane. By in situ Raman measurements the formation of pregraphitic deposits was observed for zirconia- and zirconia/alumina-supported catalysts. Hydrogen prereduction suppressed the formation of all surface species and dehydrogenation products for the alumina-containing catalysts, whereas the zirconia-supported one was less affected.

The performance of the bare supports was influenced by the Lewis acidity of the material. The zirconia deposition decreased the Lewis acidity of alumina decreasing the rate of coke deposition for zirconia/alumina compared with alumina. The addition of chromia on the supports increased the dehydrogenation activity of all materials, but the chromia/alumina catalyst was more active than the chromia/zirconia/alumina catalysts. The highest dehydrogenation activity was observed for the chromia/zirconia catalyst. In contrast to the supports, the coke deposition rate for the chromia catalysts followed the activity of the catalysts. For the dehydrogenation activity of the chromia catalysts it seems that the Lewis acidity of the support is not the only influential factor, but that the phase of the zirconia is also important.

## Acknowledgements

We gratefully acknowledge the financial support provided by the Academy of Finland and the Spanish Ministry of Education and Science (CTQ2005-02802/PPQ), and the aid provided by the European coordination action CONCORDE in organizing a researcher exchange between TKK and CSIC. We thank Dr. Arla Kytökivi, Mr. Olli Jylhä, and Ms. Heli Vuori for the preparation of the catalysts, and Mr. Markus Jönsson and Ms. Susanna Wallenius for experimental assistance. Dr. Anna Lewandowska is thanked for her help with the Raman measurements.

## References

[1] B.M. Weckhuysen, R.A. Schoonheydt, Catal. Today 51 (1999) 223–232.
[2] M.M. Bhasin, J.H. McCain, B.V. Vora, T. Imai, P.R. Pujadó, Appl. Catal. A 221 (2001) 397–419.
[3] B.M. Weckhuysen, I.E. Wachs, R.A. Schoonheydt, Chem. Rev. 96 (1996) 3327–3349.
[4] M.A. Vuurman, I.E. Wachs, D.J. Stufkens, A. Oskam, J. Mol. Catal. 80 (1993) 209–227.
[5] M. Cherian, M.S. Rao, W.-T. Yang, J.-M. Jehng, A.M. Hirt, G. Deo, Appl. Catal. A 233 (2002) 21–33.
[6] R.L. Puurunen, B.M. Weckhuysen, J. Catal. 210 (2002) 418–430.
[7] A. Hakuli, A. Kytökivi, A.O.I. Krause, Appl. Catal. A 190 (2000) 219–232.
[8] F. Cavani, M. Koutyrev, F. Trifirò, A. Bertolini, D. Ghisletti, R. Iezzi, A. Santucci, G. Del Piero, J. Catal. 158 (1996) 236–250.
[9] S. De Rossi, M.P. Casaletto, G. Ferraris, A. Cimino, G. Minelli, Appl. Catal. A 167 (1998) 257–270.
[10] S. Damyanova, P. Crange, B. Delmon, J. Catal. 168 (1997) 421–430.
[11] A.C. Faro Jr., K.R. Souza, V.L.D.L. Camorim, M.B. Cardoso, Phys. Chem. Chem. Phys. 5 (2003) 1932–1940.
[12] A.C. Faro Jr., K.R. Souza, J.G. Eon, A.A. Leitão, A.B. Rocha, R.B. Capaz, Phys. Chem. Chem. Phys. 5 (2003) 3811–3817.
[13] A. Kytökivi, E.-L. Lakomaa, A. Root, H. Österholm, J.-P. Jacobs, H.H. Brongersma, Langmuir 13 (1997) 2717–2725.
[14] M.M.V.M. Souza, D.A.G. Arando, M. Schmal, J. Catal. 204 (2001) 498–511.
[15] A.B. Gaspar, L.C. Dieguez, J. Catal. 220 (2003) 309–316.
[16] M. Fernández-García, A. Martínez-Arias, J.C. Hansom, J.A. Rodriguez, Chem. Rev. 104 (2004) 4063–4104.
[17] S.T. Korhonen, M.A. Bañares, J.L.G. Fierro, A.O.I. Krause, Catal. Today 126 (2007) 235–247.
[18] R. Burch, P.K. Loader, Appl. Catal. A 143 (1996) 317–335.
[19] R.L. Puurunen, Chem. Vap. Deposition 11 (2005) 79–90.
[20] S. Haukka, Analyst 116 (1991) 1055–1057.
[21] S.M.K. Airaksinen, M.E. Harlin, A.O.I. Krause, Ind. Eng. Chem. Res. 41 (2002) 5619–5626.
[22] A. Hakuli, A. Kytökivi, E.-L. Lakomaa, O. Krause, Anal. Chem. 67 (1995) 1881–1886.
[23] M.O. Guerrero-Pérez, M.A. Bañares, Catal. Today 113 (2006) 48–57.
[24] E. Guglieminotti, Langmuir 6 (1990) 1455–1460.

[25] E. Finocchio, G. Busca, V. Lorenzelli, R.J. Willey, J. Am. Chem. Soc., Faraday Trans. 90 (1994) 3347–3356.
[26] M. Trombetta, G. Busca, S.A. Rossini, V. Piccoli, U. Cornaro, J. Catal. 168 (1997) 334–348.
[27] E. Finocchio, G. Busca, V. Lorenzelli, R.J. Willey, J. Catal. 151 (1995) 204–215.
[28] G. Busca, J. Lamotte, J.-C. Lavvalley, V. Lorenzelli, J. Am. Chem. Soc. 109 (1987) 5197–5202.
[29] S.T. Korhonen, S.M.K. Airaksinen, A.O.I. Krause, Catal. Today 112 (2006) 37–39.
[30] D.H. William, I. Flemming, Spectroscopic Methods in Organic Chemistry, McGraw-Hill Publishing Company Limited, London, 1966, pp. 52–54.
[31] J. Pater, F. Cordona, C. Canaff, N.S. Gnep, G. Szabo, M. Guisnet, Ind. Eng. Chem. Res. 38 (1999) 3822–3829.
[32] B.M. Weckhyusen, I.E. Wachs, J. Phys. Chem. 100 (1996) 14437–14442.
[33] S. Kuba, H. Knözinger, J. Raman Spectrosc. 33 (2002) 325–332.
[34] S.M.K. Airaksinen, M.A. Bañares, A.O.I. Krause, J. Catal. 230 (2005) 507–513.
[35] V. Ermini, E. Finocchio, S. Sechi, G. Busca, S. Rossini, Appl. Catal. A 190 (2000) 157–167.
[36] S.M.K. Airaksinen, A.O.I. Krause, Ind. Eng. Chem. Res. 44 (2005) 3862–3868.
[37] G. Mul, M.A. Bañares, G.C. Cortéz, B.V. Linden, S.J. Khatib, J.A. Moulijn, Phys. Chem. Chem. Phys. 5 (2003) 4378–4383.